



## Molecular Crystals and Liquid Crystals Science and Technology. Section A. Molecular Crystals and Liquid Crystals

Publication details, including instructions for authors and  
subscription information:

<http://www.tandfonline.com/loi/gmcl19>

### Liquid Crystal Order in a Highly Restrictive Porous Glass

Germano S. Iannacchione<sup>a b</sup>, Sihai Qian<sup>a b</sup>, Gregory P. Crawford<sup>b</sup>,  
Sandra S. Keast<sup>b</sup>, Mary E. Neubert<sup>b</sup>, J. William Doane<sup>a b</sup>, Daniele  
Finotello<sup>a b</sup>, Lindsay M. Steele<sup>c</sup>, Paul E. Sokol<sup>c</sup> & Slobodan Zumer<sup>d</sup>

<sup>a</sup> Department of Physics, and Liquid Crystal Institute, Kent, OH,  
44242, USA

<sup>b</sup> Department of Physics, Kent State University, Kent, OH, 44242,  
USA

<sup>c</sup> Department of Physics, Penn State University, University Park, PA,  
16802, USA

<sup>d</sup> Department of Physics, University of Ljubljana, Jadranska, 19,  
61000, Ljubljana, Slovenia

Version of record first published: 23 Sep 2006.

To cite this article: Germano S. Iannacchione, Sihai Qian, Gregory P. Crawford, Sandra S. Keast, Mary E. Neubert, J. William Doane, Daniele Finotello, Lindsay M. Steele, Paul E. Sokol & Slobodan Zumer (1995): Liquid Crystal Order in a Highly Restrictive Porous Glass, Molecular Crystals and Liquid Crystals Science and Technology. Section A. Molecular Crystals and Liquid Crystals, 262:1, 13-23

To link to this article: <http://dx.doi.org/10.1080/10587259508033508>

PLEASE SCROLL DOWN FOR ARTICLE

Full terms and conditions of use: <http://www.tandfonline.com/page/terms-and-conditions>

This article may be used for research, teaching, and private study purposes. Any substantial or systematic reproduction, redistribution, reselling, loan, sub-licensing, systematic supply, or distribution in any form to anyone is expressly forbidden.

The publisher does not give any warranty express or implied or make any representation that the contents will be complete or accurate or up to date. The accuracy of any instructions, formulae, and drug doses should be independently verified with primary sources. The publisher shall not be liable for any loss, actions, claims, proceedings,

demand, or costs or damages whatsoever or howsoever caused arising directly or indirectly in connection with or arising out of the use of this material.

## LIQUID CRYSTAL ORDER IN A HIGHLY RESTRICTIVE POROUS GLASS

GERMANO S. IANNACCHIONE <sup>a,b</sup>, SIHAI QIAN <sup>a,b</sup>, GREGORY P.  
CRAWFORD <sup>b</sup>, SANDRA S. KEAST <sup>b</sup>, MARY E. NEUBERT <sup>b</sup>, J. WILLIAM  
DOANE <sup>a,b</sup>, DANIELE FINOTELLO <sup>a,b</sup>  
Department of Physics <sup>a</sup> and Liquid Crystal Institute <sup>b</sup>, Kent State University, Kent,  
OH, 44242, USA.

LINDSAY M. STEELE, PAUL E. SOKOL  
Department of Physics, Penn State University, University Park, PA, 16802, USA.

SLOBODAN ZUMER  
Department of Physics, University of Ljubljana, Jadranska 19, 61000 Ljubljana,  
Slovenia.

**Abstract** The thermodynamic and structural properties of octylcyanobiphenyl (8CB) confined to the highly restrictive and randomly interconnected pores of Vycor glass were studied via AC calorimetry, DSC, and small angle neutron scattering. The weakly first order nematic to isotropic phase transition is absent and replaced by a continuous evolution of local orientational ordering with decreasing temperature. The results are consistent with predictions from a model that treats the host media as a collection of noninteracting pore segments. The continuous smectic-A to nematic phase transition is also absent with no evidence of any smectic ordering. In addition, crystallization is replaced by a glass-like melting transition with indications of another melting transition at much lower temperatures.

## INTRODUCTION

The study of confinement effects on liquid crystalline ordering continues to attract considerable interest from both fundamental and applied points of view. Not only are confined liquid crystals at the heart of all display devices, but the effects of finite size and surface interactions on the numerous available phase transitions provide an enormously rich field of study. Research with different materials (helium, binary liquid mixtures, and liquid crystals among others) confined to porous structures which are randomly interconnected has recently become an area of great activity. Despite the topologically compli-

cated nature of the confining media, the complete randomness have lead to two theoretical approaches in understanding phase transitions and dynamics restricted to such substrates. These are generally based on either a "random-field" Ising (RFI) or a "single-pore" (SP) model. In the first, the system is modeled as an Ising collection of spins representing the liquid crystal that is acted upon by a Hamiltonian of randomly oriented external fields representing the effect of the confining substrate<sup>1-3</sup>. Such an approach treats the surface, the source of the random interactions, as an externally applied field that does not limit the interactions among the spins (molecules). In reality, surfaces take up volume in the sample and thus limit the interactions between molecules comprising the ordered phase. In systems where the density of the confining substrate is sufficiently low (i.e. highly interconnected voids with solid "strings") the RFI model may apply. As the density increases, true pores form and the interaction and correlations between pore regions weakens. In the SP approach<sup>4,6</sup>, the pores are treated as independent and the system becomes a collection of noninteracting pore segments where the ordering is locally determined. The randomness of the porous media is manifest in the distribution of size, shape, and surface interaction in the individual pores; the overall order is averaged over such a distribution.

Recent work on liquid crystals confined to randomly interconnected porous substrates includes light scattering and calorimetry for 8CB confined to the silica gel matrix of aerogel<sup>7</sup>. There, the density of the silica is low and the structure is that of strings of silica imbedded in the liquid crystal. The nematic to isotropic transition, becoming nearly continuous and shifted to lower temperatures, was modeled by an RFI approach. X-ray studies on the same system found that the smectic ordering smoothly increases with decreasing temperature. The experimentally determined correlation length at the smectic-A to nematic transition,  $\xi \sim 40 \text{ \AA}$ , is much smaller than the mean void size,  $\sim 200 \text{ \AA}$ . Crystallization was suppressed to  $-4 \text{ }^\circ\text{C}$  and consisting of single crystallites with no long range order within the aerogel<sup>8</sup>. However, the slow dynamics of nematic fluctuations within such porous media remains unexplained by an RFI approach<sup>9</sup>. Liquid crystals confined to a more dense media, i.e. more restrictive like Vycor glass, found no evidence of a nematic transition and instead observed a continuous increase of local orientational order with decreasing temperature<sup>10</sup>. The  $^2\text{H}$ -NMR spectra and heat capacity behavior with tempera-

ture were successfully explained by a SP model using a modified Landau-de Gennes approach to account for the local ordering/disordering within each pore, eventually averaged over a distribution of pores forming Vycor glass.

In this work, we report studies for octylcyanobiphenyl (8CB) liquid crystal confined to the 70 Å diameter pores of Vycor glass. By using AC and DS calorimetry, and small angle neutron scattering (SANS), the thermodynamic and structural properties at the weakly first order nematic to isotropic (NI), the continuous smectic-A to nematic (AN), and the first order crystal to smectic-A (KA) phase transitions are explored. An extremely broad, suppressed and shifted to lower temperature heat capacity bump is observed with both AC and DS calorimetry. In addition, with DSC, a sharp peak near 20 °C is observed on heating, having a large hysteresis on cooling, with a small latent heat. At even lower temperatures, a second, very broad, feature is observed with DSC, also having a large hysteresis and small latent heat, which may indicate the presence of another glass-like melting transition. In all calorimetric experiments, no evidence of a NI or AN transition is found. Curiously, a SANS peak characteristic of the Vycor glass is found to suddenly increase in intensity near 20 °C. Coupled with the DSC observations, this may be an indication of a transition where the liquid crystal molecules melt from a glassy state induced by the host substrate.

## EXPERIMENTAL DETAILS

Vycor, a Corning trademark, is a high purity silicon-oxide glass made by a spinodal decomposition of SiO<sub>2</sub> and other oxides (mainly boric oxide). After cooling, these other oxides are leached away by an acid bath. The remaining SiO<sub>2</sub> forms a quasi-periodic interconnected arrangement of pore segments, ~ 70 Å in diameter and ~ 300 Å in length, with a 28 % porosity. Over the wide temperature range studied in this work, the glass is characterized by an extremely weak temperature dependence in both heat capacity and thermal expansivity. The samples are prepared by thoroughly cleaning the glass in a 30 % hydrogen-peroxide bath at 100 °C for 4 to 6 hours, then rinsed with distilled water several times before drying in a vacuum oven at 90 °C for 24 hours. The clean glass is then immersed in an isotropic bath of 8CB (at ~ 47 °C) for 24 hours, the excess liquid crystal is

removed by pressing the glass between sheets of highly absorbent Whatman filter paper. Mass measurements before and after this process indicate that complete filling of the pore network was achieved. The 8CB used throughout this study has been deuterated in the first carbon position of the alkyl chain ( $\alpha$  position) and purified to better than 99.9 %. This liquid crystal has three phase transitions, a first order KA at  $\sim 21$  °C, a continuous AN at 33.5 °C, and a weakly first order NI at 40.5 °C with latent heats of  $I_{KA} = 97.1$  J/g,  $I_{AN} = 0.00137$  J/g, and  $I_{NI} = 2.1$  J/g respectively <sup>11</sup>.

High resolution heat capacity measurements were performed using AC calorimetry. It consists of applying heat sinusoidally to a sample and measuring the amplitude of the resulting thermal oscillations which are inversely proportional to its heat capacity. The amplitude of the temperature oscillations was typically 2 mK with data taken at discrete temperature steps spaced by 20 mK; the average temperature was controlled to better than 100  $\mu$ K. Details of our implementation of this technique can be found elsewhere <sup>12</sup>. The sample consisted of a 18.6 mg glass chip containing 2.9 mg of 8CB. Measurements were also performed on the empty Vycor glass which, along with the rest of the addendum heat capacity, was subtracted from measurements made with the filled sample.

Differential scanning calorimetry was performed using a Perkin-Elmer DSC 7. Two equal mass ( $\approx 15$  mg) Vycor glass pieces were shaped to fit snugly into the aluminum pans of the DSC. One was left empty and used in the reference cell while the second was filled with 8CB ( $\sim 2.5$  mg) and placed in the sample cell. In such an arrangement, the glass contribution is directly subtracted from the thermal scans. After slowly cycling the sample over the temperature range of interest, -25 to 50 °C, then waiting one hour at the starting temperature, two sets of heating and cooling scans were performed at 5 °C/min and 10 °C/min rates. Because of the small mass of 8CB, slower scanning rates resulted in a severe reduction of signal to noise.

Small angle neutron scattering (SANS) measurements were performed at the Intense Pulsed Neutron Source (IPNS) facility of the Argonne National Laboratory. The sample consisted of a  $40 \times 9 \times 1.5$  mm slab of cleaned Vycor glass containing 0.144 g of deuterated 8CB which was then sealed in a quartz holder. The scattering intensity,  $S(q)$ , as a function of momentum transfer  $q$  at 20, 22, 22.4, and 24.5 °C were recorded. Temperature control was achieved using a single stage oven with  $\sim 0.1$  °C stability.

## RESULTS AND DISCUSSION

The AC heat capacity measurements on 8CB confined to Vycor are presented in Figure 1. Over a temperature range bracketing the bulk AN and NI transitions, no evidence of any phase transition is found, however, the heat capacity exhibits a stronger temperature dependence than bulk near and above  $T_{NI}$ . This may be due to some additional background contribution induced by the confining substrate. After subtraction of the high temperature heat capacity behavior extrapolated to lower temperatures, a broad and very suppressed bump, centered several degrees *below* the bulk AN transition, is seen.

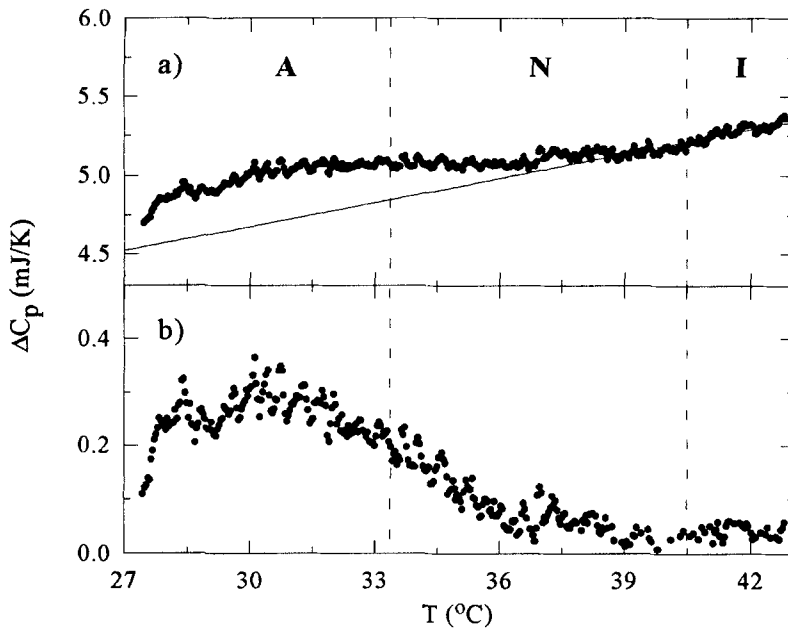


FIGURE 1 Heat capacity as a function of temperature bracketing the AN and NI phase transition indicated by the vertical dashed lines. a)  $C_p$  of 8CB confined to Vycor showing the temperature dependence near and above  $T_{NI}$ . b)  $\Delta C_p$  after subtraction of the high temperature behavior given by the solid line in a).

Similar behavior was previously found for 5CB and 7CB (liquid crystals with only a nematic phase) confined to Vycor, and is interpreted as a continuous evolution of local orientational order which increases with decreasing temperature<sup>10</sup>. Since no evidence for the AN transition is found, it is concluded that smectic ordering is highly suppressed or completely absent. Considering the smectic layer spacing for 8CB is  $\sim 30$  Å, it is not surprising that smectic ordering would be absent within 70 Å size pores. Under confinement

conditions, and likely due to severe elastic distortions, the smectic ordering is at most short ranged<sup>8,15</sup>.

The orientational ordering can be understood by modeling this system using a SP approach given that the length to width ratio is  $l/d \sim 4$ . Assuming that the director within each pore is along the long axis of the pore, homogeneous alignment, and that the orientational order can be described by a scalar order parameter,  $Q$ , averaged over the pore, then, the free energy for a single pore can be written as,

$$f = f_o + \frac{1}{2}a(T - T^*)Q^2 - \frac{1}{3}bQ^3 + \frac{1}{4}cQ^4 + hQ^2 - gQ \quad (1)$$

where  $f_o$ ,  $a$ ,  $T^*$ ,  $b$ , and  $c$  are known phenomenological parameters. The last two terms represent the confinement-induced disorder and order respectively. The minimization of Eq. (1) yields the temperature dependence of  $Q$ . Such a free energy has been employed for less restrictive confined systems to model surface interactions<sup>13</sup>.

The  $hQ^2$  term is the disordering effects of the topology-induced deformations resulting from the randomly interconnected pore network structure. As such,  $h$  should vary from pore to pore and can be approximated by,  $h \sim L/R^2$ , where  $L$  is the Landau-de Gennes expansion coefficient for all terms having derivatives of  $Q$  in second order and  $R$  is an effective radius of curvature. The  $-gQ$  term represents ordering effects of the surface interaction and should only depend on the surface anchoring strength, thus a constant over the porous network. The coefficient  $g$  can be estimated by  $g = W/(RS_{nem})$  where  $W$  is the surface anchoring strength and  $S_{nem}$  the bulk nematic order parameter.

The randomness of the porous media is introduced by a Gaussian distribution,  $\omega(h)$ , characterized by an average  $h_o$  and width  $\sigma$ , of the disordering coefficient arising from a distribution of effective radii of curvature. Once  $Q$  is known for a given  $h$ , it is then averaged over the distribution yielding the average orientational order,  $\langle Q \rangle$ , of the system. From <sup>2</sup>H-NMR measurements on deuterated 5CB in Vycor<sup>10</sup>, the linewidth of the single, broad, absorption peak is a direct measure of  $\langle Q \rangle$ . Given phenomenological parameters for 5CB and the surface anchoring strength of 5CB on SiO<sub>2</sub> ( $W = 10^4$  J/m<sup>2</sup>), fits of  $\langle Q \rangle$  using Eq. (1) yield  $h_o$  and  $\sigma$ , the only adjustable parameters. Once the  $\langle Q \rangle$  temperature dependence is known, the excess heat capacity due to the orientational ordering



can be calculated from <sup>14</sup>

$$\Delta C_p = aVT \left\langle Q \frac{\partial Q}{\partial T} \right\rangle \quad (2)$$

where  $V$  is the open volume of the pore network. The model predicted  $\Delta C_p$  is shown in Figure 2 and is in excellent agreement with the measured excess heat capacity <sup>10</sup> and closely resembles the observed heat capacity of 8CB in Vycor.

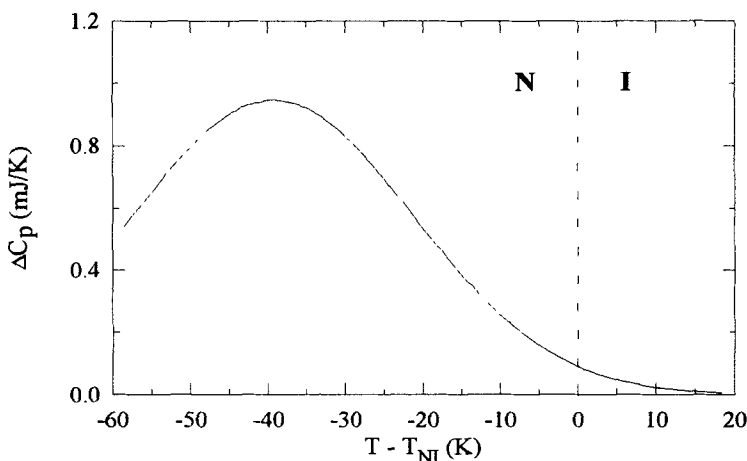


FIGURE 2 Theoretical excess heat capacity,  $\Delta C_p$ , due to orientational ordering for 5CB confined to Vycor glass.

DSC measurements also show a broad and suppressed bump centered below the bulk  $T_{NI}$ , in both heating and cooling scans, with a hysteresis of  $\sim 4^\circ\text{C}$  at a scanning rate of  $5^\circ\text{C}/\text{min}$ . See Figure 3. The hysteresis of this bump increases to only  $\sim 5^\circ\text{C}$  when the scanning rate doubles to  $10^\circ\text{C}/\text{min}$ . Its area,  $\sim 3 \text{ J/g}$ , compares well with the latent heat of the bulk NI transition of  $2.1 \text{ J/g}$ . The latent heat results combined with the lack of a sharp heat capacity feature supports the view that the weakly first order NI transition has become a glass-like transition which involves the freezing of the orientational order within the pore network.

The DSC measurements, extending to  $-25^\circ\text{C}$ , also found a sharp feature near the bulk KA transition upon heating, but is supercooled by  $28^\circ\text{C}$  upon cooling, having an area of  $\sim 1.5 \text{ J/g}$ . At lower temperatures, near  $0^\circ\text{C}$  on heating, another, very broad feature is observed, also showing large hysteresis effects,  $\sim 21^\circ\text{C}$ , with an area of  $\sim 10.5 \text{ J/g}$ .

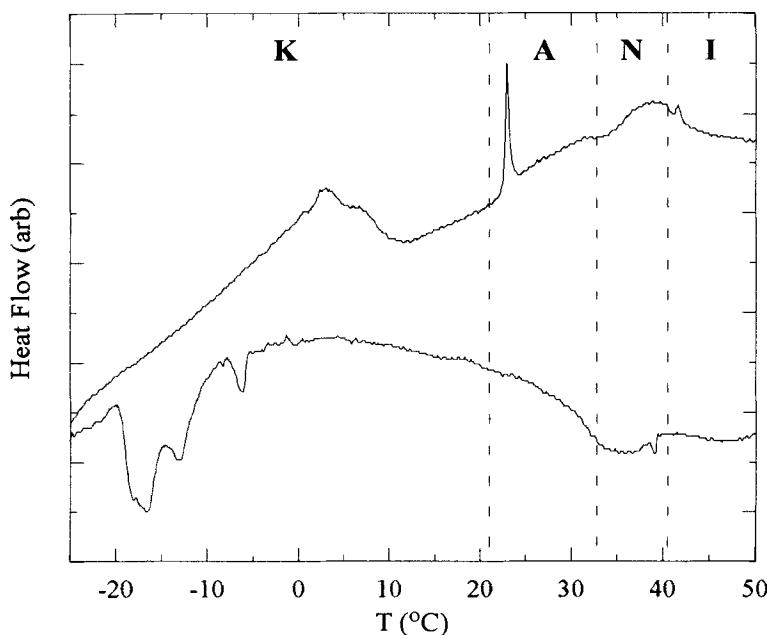


FIGURE 3 DSC curves of 8CB confined to Vycor glass at 5 °C/min. The upper trace is a heating scan while the lower trace is a cooling scan and the vertical dashed lines indicate the bulk transitions. Note the broad bump below  $T_{NI}$  also seen by AC calorimetry.

Despite the small sample size and the fact that DSC measurements generally overestimate the true latent heat, both features have a latent heat at least an order of magnitude smaller than that of the bulk crystallization (97.1 J/g). Combining the large hysteresis effects and the small latent heats, these two features probably reflect melting transitions where the liquid crystal, in some glassy state, unbinds from the confining substrate in two stages. Although first order crystallization transitions under confinement are known to be greatly suppressed<sup>16</sup>, here, the highly restrictive confinement appears to convert the KA transition into one, possibly two, solid-glass transitions. Evidently, studies that probe the liquid crystal structure at these temperatures are needed.

SANS measurements, which took place prior to the DSC work, were performed at a few temperatures just below and above the bulk KA transition in order to probe the structural properties of the confined liquid crystal. Figure 4 shows the scattering intensity,  $S(q)$ , as a function of momentum transfer  $q$  from 0.003 to 0.35 Å<sup>-1</sup> at 20, 22, 22.4, and 24.5 °C. A broad peak is observed at all temperatures at  $q = 0.01765$  Å<sup>-1</sup>, which corre-

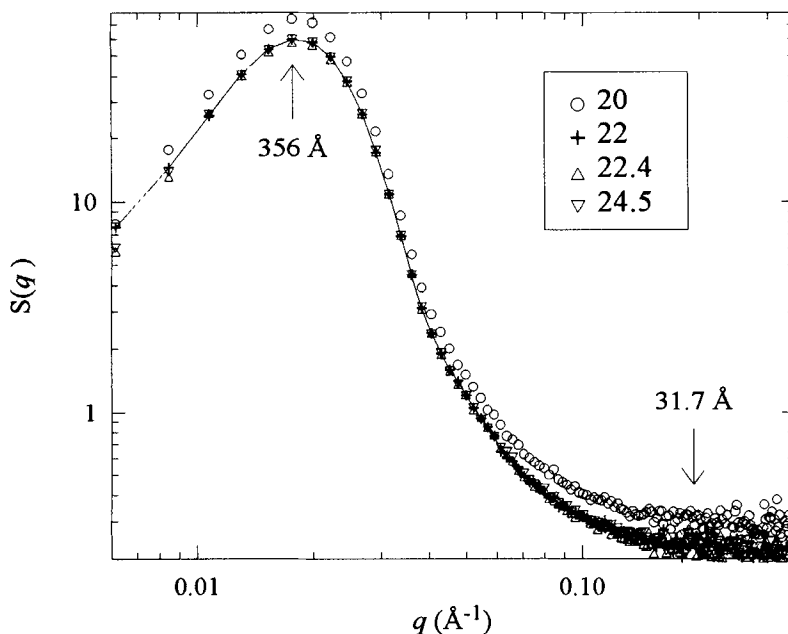


FIGURE 4 SANS data plotted as a function of  $q$  on a log-log scale for the four temperatures studied. Note that the 22, 22.4, and 24.5 °C, the scans overlay each other perfectly. At 20 °C, just below the bulk KA transition, the intensity is larger for all  $q$ . Solid line is an average for the three highest temperature scans and the arrows indicate dimensions for the Vycor glass peak maximum (356 Å) and the expected smectic layer spacing (31.7 Å) of bulk 8CB.

sponds to a spacing of  $d = 2\pi/q = 356$  Å, is well known to be characteristic of the quasi-periodic pore-solid structure of Vycor glass<sup>17</sup>. No indication of smectic ordering, expected to occur at  $q = 0.198$  Å<sup>-1</sup> ( $d = 31.7$  Å, the expected 8CB smectic layer spacing)<sup>18</sup>, or crystal features which should appear in the range of  $0.48 < q < 1.4$  Å<sup>-1</sup> (not shown in Figure 4) are found.

For the three highest temperatures, the scattering data nicely overlaps, however, at 20 °C, in the immediate vicinity of the sharp peak observed by DSC, there is an increase in  $S(q)$  at all  $q$ . Given the narrow temperature range, such a change is entirely due to the imbedded liquid crystal and is interpreted as an increase in the density of the deuterated liquid crystal within the pore structure. Since no crystal features were observed and the latent heat is small, this increase in density is due to a glassy transition occurring near the bulk KA transition where the orientationally frozen nematic-like 8CB freezes into a glass-like amorphous solid mimicking the Vycor glass.

## CONCLUSIONS

We have undertaken a detailed study of 8CB confined to Vycor glass using AC and DS calorimetry, and SANS techniques, which explored the thermodynamic and structural properties of the three ordered phases: nematic, smectic-A, and crystal. No evidence of a NI, AN or KA transition is found. A broad and suppressed bump centered at  $\sim 31$  °C is observed by both AC and DS calorimetry which indicates a continuous evolution of local orientational order with decreasing temperature. This behavior is understood in terms of a "single-pore" model developed to explain the behavior of nematics confined to highly restrictive and randomly interconnected porous media<sup>10</sup>. SANS results finds that no smectic nor crystal order occurs down to 20 °C. Instead, at this temperature there is an increase in scattering intensity at all  $q$  indicating an increase in density of liquid crystal molecules within the pores. At nearly the same temperature, DSC scans show a hysteretic sharp feature having a small latent heat. We speculate that a glass-like transition takes place where the liquid crystal goes from an orientationally frozen state to a translationally frozen state with a structure that mimics that of the amorphous solid (Vycor glass). A possible second glass-like transition occurs near 0 °C.

Further work is needed to better characterize the structure of the liquid crystal solid phase by extending the SANS experiments to lower temperature and higher  $q$ . Measurements by  $^2\text{H}$ -NMR would shed light onto the orientational ordering and relaxation dynamics. Light scattering experiments would also be useful in relaxation dynamics studies as well as providing structural information characterizing the glassy state near and below the bulk KA transition.

## ACKNOWLEDGMENTS

We gratefully thank J. T. Mang and S. Kumar for many useful discussions. This work at KSU was supported by the NSF-STC ALCOM grant No. DMR 89-20147, NSF Solid State Chemistry grant No. 91-20130, and the ALCOM Resource Facility. At PSU, support was through NSF grant No. DMR 91-23469. We also benefited from the use of the IPNS at Argonne National Laboratory funded by DOE, BES-Material Science under contract W-31-109-Eng.-38.

**REFERENCES**

1. F. Brochard and P.G. de Gennes, J. Phys. Lett., **44**, 785 (1983); P.G. de Gennes, J. Phys. Chem., **88**, 6469 (1984).
2. Y.Y. Goldsmitd and A. Aharony, Phys. Rev. B, **32**, 264 (1985).
3. K. Binder and A.P. Young, Rev. Mod. Phys., **58**, 801 (1986).
4. A.J. Liu, J. Durian, E. Herbolzheimer, and S.A. Safran, Phys. Rev. Lett., **65**, 1897 (1990).
5. A.J. Liu and G.S. Grest, Phys. Rev. A, **44**, 7879 (1991).
6. L. Monette, A.J. Liu, and G.S. Grest, Phys. Rev. A, **46**, 7664 (1992).
7. T. Bellini, N.A. Clark, C.D. Muzny, L. Wu, C.W. Garland, D.W. Schaefer, and B.J. Oliver, Phys. Rev. Lett., **69**, 788 (1992).
8. N.A. Clark, T. Bellini, R.M. Malzbender, B.N. Thomas, A.G. Rappaport, C. D. Muzny, D.W. Schaefer, and L. Hrubesh, Phys. Rev. Lett., **71**, 3505 (1993).
9. X.-L. Wu, W.I. Goldberg, M.X. Liu, and J.Z. Xue, Phys. Rev. Lett., **69**, 470 (1992).
10. G.S. Iannacchione, G.P. Crawford, S. Zumer, J.W. Doane, and D. Finotello, Phys. Rev. Lett., **71**, 2595 (1993).
11. J. Thoen, H. Marynissen, and W. Van Dael, Phys. Rev. A, **26**, 2886 (1982).
12. L.M. Steele, G.S. Iannacchione, and D. Finotello, Rev. Mex. de Fis., **39**, 588 (1993).
13. P. Sheng, Phys. Rev. A, **26**, 1610 (1982); P. Sheng, Phys. Rev. Lett., **37**, 1059 (1976).
14. M. A. Anisimov, Mol. Cryst. Liq. Cryst., **162A**, 1 (1988).
15. G.S. Iannacchione and D. Finotello, Phys. Rev. Lett., **69**, 2094 (1992); and submitted to Phys. Rev. E.
16. J. Warnock, D.D. Awschalon, and M.W. Shafer, Phys. Rev. Lett., **57**, 1753 (1986).
17. M.Y. Lin, S.K. Sinha, J.M. Drake, X.-L. Wu, P. Thiyaganajan, and H.B. Stanley, Phys. Rev. Lett., **72**, 2207 (1994).
18. D. Davidov, C.R. Safinya, M. Kaplan, R. Schaetzing, R.J. Birgenau, and J.D. Litster, Phys. Rev. B, **19**, 1657 (1979).